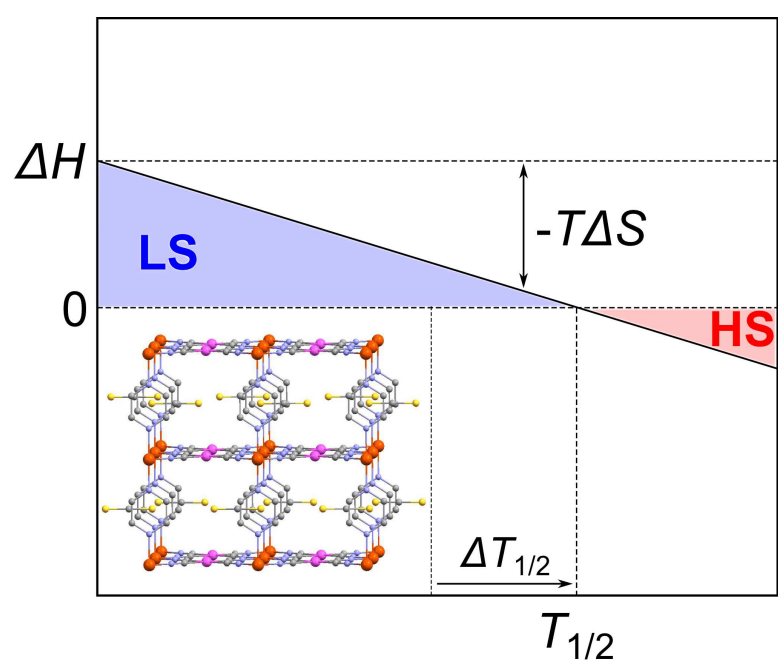
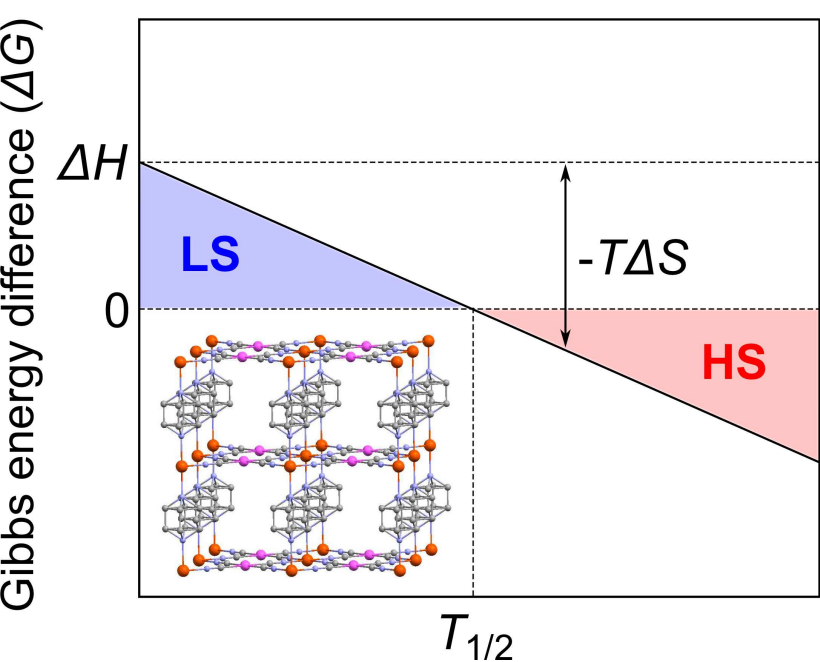


Highlights

First study on the mechanism of guest-induced spin transition

Large entropy difference in the porous coordination polymer between low and high spin states

Decrease in the entropy difference in CS₂ clathrate induces high to low spin transition



1
2
3
4
5
6
7
8
9 Theoretical Study on High-Spin to Low-Spin Transition
10 of $\{\text{Fe}(\text{pyrazine})[\text{Pt}(\text{CN})_4]\}$: Guest-Induced Entropy
11 Decrease
12
13

14 Hideo Ando^a, Yoshihide Nakao^a, Hirofumi Sato^a, Masaaki Ohba^b, Susumu
15 Kitagawa^c, Shigeyoshi Sakaki^{d,*}
16

17 ^a*Department of Molecular Engineering, Graduate School of Engineering, Kyoto University,*
18 *Nishikyo-ku, Kyoto 615-8510, Japan*

19 ^b*Department of Chemistry, Graduate School of Sciences, Kyushu University, Hakozaki*
20 *Higashi-ku, Fukuoka 812-8581, Japan*

21 ^c*Department of Synthetic Chemistry and Biological Chemistry, Graduate School of*
22 *Engineering, Kyoto University, Nishikyo-ku, Kyoto 615-8510, Japan*

23 ^d*Fukui Institute for Fundamental Chemistry, Kyoto University, Takano-Nishihiraki-cho,*
24 *Sakyo-ku, Kyoto 606-8103, Japan*
25
26

27
28 **Abstract**
29

30 A porous coordination polymer (PCP), $\{\text{Fe}^{\text{II}}(\text{pyrazine})[\text{Pt}^{\text{II}}(\text{CN})_4]\}$, adsorbs
31 CS_2 molecules to induce spin transition from high-spin (HS) to low-spin (LS)
32 state. To elucidate this mechanism, we investigated flexibility of the PCP frame-
33 work, namely rotation of pyrazine ligands, with DFT method and evaluated the
34 rotational entropy difference (ΔS_{rot}^{HS-LS}) between the HS and LS states with
35 Fourier grid Hamiltonian method. The ΔS_{rot}^{HS-LS} value is considerably large in
36 the absence of CS_2 . The CS_2 adsorption occurs between two pyrazine ligands
37 to suppress the pyrazine rotation in both states, which decreases ΔS_{rot}^{HS-LS} to
38 induce the HS \rightarrow LS transition at room temperature.
39
40
41
42
43
44
45
46
47
48
49

50
51
52 *Corresponding author. Tel: +81 75 7117907. Fax: +81 75 7114757.

53 *Email addresses:* hideo@tich14.mbox.media.kyoto-u.ac.jp (Hideo Ando),
54 nakao.yoshihide.5a@kyoto-u.ac.jp (Yoshihide Nakao), hirofumi@moleng.kyoto-u.ac.jp
55 (Hirofumi Sato), ohba@chem.kyushu-univ.jp (Masaaki Ohba),
56 kitagawa@icems.kyoto-u.ac.jp (Susumu Kitagawa),
sakaki@qmst.mbox.media.kyoto-u.ac.jp (Shigeyoshi Sakaki)
57
58

1. Introduction

One of the authors (M. O.) and his colleagues recently found that a porous coordination polymer (PCP), $\{\text{Fe}^{\text{II}}(\text{pz})[\text{Pt}^{\text{II}}(\text{CN})_4]\}$ (pz = pyrazine, Figure 1a) [1, 2, 3], adsorbs various guest molecules to induce spin transition between the LS (singlet) and the HS (quintet) states at room temperature [4]. For instance, LS \rightarrow HS transition is induced by adsorption of guest species whose size or occupation number per pore is large in many cases. This transition is understood by steric repulsion between bulky guests and the PCP framework [4], as follows. The steric repulsion is smaller in the HS framework than in the LS one because the HS framework is larger than the LS one [3, 4]. Hence, the HS framework is favorable for adsorption of bulky guests. This is the reason why the LS \rightarrow HS transition is induced by bulky guests. In the case of adsorption of CS₂, on the other hand, reverse HS \rightarrow LS transition is unexpectedly induced. The reason of this reverse transition is not clear at all.

In general, the HS \rightarrow LS transition occurs when temperature goes down to the spin transition temperature ($T_{1/2}$). Hence, the CS₂-induced HS \rightarrow LS transition corresponds to the fact that $T_{1/2}$ becomes higher by CS₂ adsorption; in fact, the $T_{1/2}$ of the CS₂ clathrate ($T_{1/2} > 330$ K) is higher than that of the guest-free framework ($T_{1/2}^{\downarrow} = 285$ K and $T_{1/2}^{\uparrow} = 309$ K) [4], where $T_{1/2}^{\downarrow}$ means $T_{1/2}$ in cooling and vice versa. In a non-cooperative model [5] or several cooperative models [5, 6], $T_{1/2}$ is described as

$$T_{1/2} = \frac{\Delta H^{HS-LS}}{\Delta S^{HS-LS}}. \quad (1)$$

1
2
3
4
5
6
7
8
9 This shows that $T_{1/2}$ shifts to higher temperature when enthalpy difference
10 (ΔH^{HS-LS}) increases and/or entropy difference (ΔS^{HS-LS}) decreases. We
11 omit the superscript “ $HS - LS$ ” for brevity hereafter.
12
13

14
15 When PCP adsorbs guest molecules, van der Waals (vdW) interaction and
16 also steric repulsion are formed between guest molecules and the PCP frame-
17 work. It is of considerable interest to clarify how these local perturbations
18 induce drastic change in macroscopic properties such as ΔS , ΔH , and $T_{1/2}$ in
19 the guest-induced spin transition of $\{\text{Fe}^{\text{II}}(\text{pz})[\text{Pt}^{\text{II}}(\text{CN})_4]\}$. In this study, we
20 aim to investigate the influence of CS_2 adsorption on ΔS , ΔH , and $T_{1/2}$ and
21 elucidate the mechanism through which the CS_2 -induced HS \rightarrow LS transition oc-
22 curs in $\{\text{Fe}^{\text{II}}(\text{pz})[\text{Pt}^{\text{II}}(\text{CN})_4]\}$.
23
24
25
26
27
28
29
30
31
32
33

34 **2. Models and theoretical methods**

35
36

37 In guest-free LS and HS frameworks of $\{\text{Fe}^{\text{II}}(\text{pz})[\text{Pt}^{\text{II}}(\text{CN})_4]\}$, disorder of pz
38 ligands was observed in the X-ray diffraction measurement (Figure 1a) [4]. This
39 implies that the pz ligands rotate around the Fe – Fe axes in both LS and HS
40 frameworks. In CS_2 clathrate, the PCP adsorbs CS_2 molecules between two pz
41 ligands and the disorder disappears (Figure 1b) [4]. This indicates that the pz
42 rotation can be strongly suppressed by the CS_2 adsorption. Except for the pz
43 rotation, such vibrational motions as stretching and bending modes are involved.
44 It is, however, likely that these motions are not influenced very much by the
45 CS_2 adsorption because this CS_2 adsorption occurs through vdW interaction
46 between CS_2 and the PCP framework [4]. We hence investigated the influence
47
48
49
50
51
52
53
54
55
56
57
58

1
2
3
4
5
6
7
8
9 of the CS₂ adsorption on ΔS and ΔH in terms of the pz rotation.

10
11 Hindered rotational entropies (S_{rot}) and internal energies (U_{rot}) were eval-
12 uated through the following three steps. First, potential energy curves (PECs)
13 of pz rotation in the LS and the HS frameworks were calculated. We employed
14 two local structure models, namely vertical and parallel models (Figures 2a and
15 2b). Both models consist of two square-planar [Fe(NC)₄]²⁻ anions and three pz
16 ligands, whose geometries were taken to be the same as the experimental ones
17 (**1** · 2H₂O(LS) and **1** · 2H₂O(HS) in Ref. [4]). Point charges (PC^{Pt}) of +0.5
18 e are placed to mimic Pt atoms. In the vertical (or parallel) model, the top
19 and the bottom pz ligands are fixed vertical (or parallel) with each other and
20 only middle pz ligand rotates around the Fe – Fe axis. The rotation angle θ
21 (Figure S1) was employed as a coordinate with the rigid-rotor approximation
22 for the pz ligand. When the rotating pz ligand is parallel with the top pz ligand,
23 the angle $\theta = 0$. Along the coordinate, the PECs of the LS and the HS states
24 were evaluated with the DFT(B3LYP) method [7, 8, 9] in Gaussian 03. In an
25 octahedral (O_h) structure around the Fe center, the LS state has no orbital
26 degeneracy (¹ A_{1g}). Though there are three near-degenerate sub-states in the
27 HS state, corresponding to ⁵ T_{2g} in O_h group, it is likely that the three PECs
28 of those sub-states are close to each other because the PECs of the pz rotation
29 mainly depend on steric repulsion with cyanide ligands (CN⁻), as will be dis-
30 cussed below. We hence calculated only one PEC for each spin state. For Fe
31 atom, the (311111/22111/411/1) basis set [10] was employed with the effective
32 core potentials of the Stuttgart group. For N, C, and H atoms in pz ligands and
33
34
35
36
37
38
39
40
41
42
43
44
45
46
47
48
49
50
51
52
53
54
55
56
57
58
59
60
61
62
63
64
65

1
2
3
4
5
6
7
8
9 for N and C atoms in CN^- ligands, the cc-pVDZ basis sets [11] and the aug-cc-
10 pVDZ basis sets [11, 12] were used, respectively. Potential energy barriers for
11 the pz rotation were investigated in detail with a smaller model which includes
12 only one Fe atom (Figures 2c). The geometry of the smaller model was taken
13 to be the same as the LS geometry of $\mathbf{1} \cdot 2\text{H}_2\text{O}(\text{LS})$ [4]. To investigate the effect
14 of the Fe – pz bonding interaction on the energy barriers, NH_3 was employed
15 instead of one pz ligand in the small model. In this NH_3 model (Figure 2d), the
16 distance between the N and the Fe atoms is taken to be 2.035 Å, which is the
17 equilibrium Fe – NH_3 distance in the LS state.
18
19
20
21
22
23
24
25
26
27

28 Then, quantized rotational energy levels (E_i) were calculated with the rota-
29 tional Schrödinger equation in the vertical model.
30
31

$$\left(-\frac{\hbar^2}{2I_\theta} \frac{\partial^2}{\partial \theta^2} + \hat{V}(\theta) \right) \Psi_i(\theta) = E_i \Psi_i(\theta), \quad (2)$$

32 where \hat{V} represents the PECs calculated above. The N – N (or Fe – Fe) axis is
33 a principal axis of inertia of the pz ring, where the principal moment of inertia
34 (I_θ) is 276.50 amu Bohr² for the LS framework and 285.68 amu Bohr² for the
35 HS one. Note that the principal axes and moments of inertia of the pz ring
36 were obtained by diagonalizing the inertia tensors for the pz structures in the
37 experimental LS and HS geometries. To solve Eq. 2, we employed the Fourier
38 grid Hamiltonian method [13] with the grid space of $\Delta\theta = \pi/1000$ rad and the
39 cubic spline interpolation.
40
41
42
43
44
45
46
47
48
49
50
51

52 Finally, the hindered rotational entropies (S_{rot}) and internal energies (U_{rot})
53 in the LS and the HS frameworks and their differences (ΔS_{rot} and ΔU_{rot}) were
54
55
56
57
58
59
60
61
62
63
64
65

1
2
3
4
5
6
7
8
9 obtained within the canonical ensemble formalism.

$$S_{rot} = \frac{\partial (\beta^{-1} \ln Q)}{\partial T} \quad (3)$$

10
11
12
13
14 and

$$U_{rot} = -\frac{\partial (\ln Q)}{\partial \beta}, \quad (4)$$

15
16
17
18
19 where T , β , and Q are temperature, inverse temperature, and partition function,
20
21 respectively. If each pz ligand independently rotates, the partition function can
22
23 be simply described with molecular partition function.
24

$$Q = \left(\sum_{i=1}^{N_{basis}} \exp(-\beta E_i) \right)^{N_A}, \quad (5)$$

25
26
27
28
29 where N_A and N_{basis} are the Avogadro constant and the number of basis func-
30
31 tions for the Fourier grid Hamiltonian method (= 2000), respectively.
32

33
34 We also investigated how much ΔH is influenced by the vdW interaction
35
36 between CS_2 and the PCP framework [4]. The PECs of the vdW interaction
37
38 were evaluated by the CCSD(T) method with the counterpoise correction [14].
39
40 Two local structure models were employed to mimic guest-interaction sites in
41
42 the framework (Figure 1); one S atom of CS_2 is placed between two pz ligands
43
44 (site A) and the other S atom is between the four-coordinate Pt centers (site
45
46 B). For full details of the methods employed here, see Schemes S2 and S3 in our
47
48 previous paper [4].
49
50
51
52
53
54
55
56
57
58
59
60
61
62
63
64
65

3. Results and discussion

3.1. Hindered rotation of pyrazine ligands

The PECs of pz rotation in the vertical and the parallel models are shown in Figures 3a and S2. Both models provide similar PECs, showing that each pz ligand independently rotates. This means that Eq. 5 can be employed here. When the pz ligand is parallel to the Fe–NC bonds ($\theta = \pi/4$ and $3\pi/4$ rad), the potential energy becomes maximum. When the pz ligand and Fe–NC bonds are staggered ($\theta = 0$ and $\pi/2$ rad), it becomes minimum. The barrier height is $6.0 \text{ kcal mol}^{-1}$ in the LS framework and $1.1 \text{ kcal mol}^{-1}$ in the HS one (Figure 3a). These moderate values indicate that pz ligand can rotate in the guest-free framework, which results in dynamical disorder of the X-ray diffraction structure (Figure 1a). It is noted that the barrier height is larger in the LS framework than in the HS one. Hence, the pz ligand rotates much easier in the HS framework than in the LS one, indicating that ΔS_{rot} ($= \Delta S_{rot}^{HS-LS}$) is positive, as will be shown below in detail. The rotation of pz ligands was also confirmed by preliminary experimental measurement of solid-state $^2\text{HNMR}$ spectra of $\{\text{Fe}^{\text{II}}(\text{d}_4\text{-pz})[\text{Pt}^{\text{II}}(\text{CN})_4]\}$ ($T_{1/2}^\downarrow = 288 \text{ K}$ and $T_{1/2}^\uparrow = 303 \text{ K}$) using deuterated pyrazine ($\text{d}_4\text{-pz}$). The line shape of the $\text{d}_4\text{-pz}$ was simulated as four site flip of pz rings along the C_4 axis, and the pz rotational rate was estimated to be over 10^8 Hz for the HS state at 290 K and $5 \times 10^5 \text{ Hz}$ for the LS state at 260 K . The origin of the energy barriers will be discussed in Sec 3.4.

The pz rotational entropy was evaluated with Eqs. 3 and 5. As shown in Figure 4, the difference in the pz rotational entropy (ΔS_{rot}) between the HS

1
2
3
4
5
6
7
8
9 and the LS frameworks is positive in all temperatures, as suggested above. The
10 temperature dependence of ΔS_{rot} is not large at sufficiently high temperature
11 (200 K to 400 K) where spin transition is observed. Hence, an averaged ΔS_{rot}
12 value (1.84 cal mol⁻¹ K⁻¹) from 200 K to 400 K is employed to evaluate the
13 $T_{1/2}$ shift in Sec. 3.3. The difference in rotational internal energy (ΔU_{rot}) was
14 evaluated with Eqs. 4 and 5. The absolute value of the difference is smaller
15 than 0.1 kcal mol⁻¹ (see Figure S3).
16
17
18
19
20
21
22
23
24
25

26 *3.2. CS₂ adsorption and its influence on enthalpy difference*

27
28 CS₂ molecules are adsorbed to the PCP framework through vdW interaction
29 [4]. The PECs at sites A and B are shown in Figure 5, where pz ligands are
30 parallel with each other (Figure 1b). These PECs are attractive and show
31 minima between r_{LS} and r_{HS} values, where r_{LS} and r_{HS} represent the distances
32 in the experimental LS and HS frameworks, respectively.
33
34
35
36
37

38 The enthalpy change for spin transition is approximately expressed by Eq.
39 6 [15, 16, 17].
40
41

$$42 \quad \Delta H \approx \Delta E_{el} + \Delta U_{vib}, \quad (6)$$

43 where ΔE_{el} and ΔU_{vib} are potential energy difference and vibrational internal
44 energy difference between the HS and the LS states, respectively. Note that
45 this is a solid system, and hence $p\Delta V \approx 0$ [16, 17]. The CS₂ adsorption to
46 the framework little influences ΔE_{el} , as described below: (1) Binding energy
47 difference ΔBE ($= \Delta BE^{HS-LS}$) at site A (0.2 kcal mol⁻¹) and at site B (-0.4
48 kcal mol⁻¹) are very small and canceled out with each other (Figure 5). And,
49
50
51
52
53
54
55
56
57
58

1
2
3
4
5
6
7
8
9 (2) the vdW interaction little induces charge transfer from CS₂ to the Fe center,
10 which little changes the ligand field strength around the Fe center. In addition,
11 ΔU_{rot} , which is one component of ΔU_{vib} , is small as discussed in Sec. 3.1 and
12 the influence of CS₂ adsorption on ΔU_{rot} also may be small. Consequently, it
13 is likely that
14
15
16
17
18

$$\Delta H_{\text{guest-free}} \approx \Delta H_{\text{CS}_2 \text{ clathrate}}. \quad (7)$$

19
20
21
22 An averaged binding energy is 4.2 and 5.5 kcal mol⁻¹ at sites A and B, re-
23 spectively. Furthermore, the potential energy minima at sites A and B are found
24 between r_{LS} and r_{HS} , as discussed above. Because of this binding interaction,
25 the CS₂ adsorption suppresses the pz rotation in both LS and HS frameworks.
26 Note that if pz ligands rotate in CS₂ clathrate, significantly large loss of the
27 binding energy occurs because steric repulsion is formed or vdW interaction is
28 weakened. This is consistent with the fact that the disorder of pz ligands disap-
29 pears through the CS₂ adsorption (Figure 1b). In the next section, hence, we
30 discuss the influence of pz rotational entropy on the $T_{1/2}$ shift.
31
32
33
34
35
36
37
38
39
40
41
42

43 *3.3. Spin transition temperature*

44
45 We evaluated the CS₂-induced $T_{1/2}$ shift with Eq. 1. As discussed above, the
46 rotational entropy difference (ΔS_{rot}) is positive and considerably large (about
47 1.84 cal mol⁻¹ K⁻¹) in the absence of CS₂. In the presence of CS₂, CS₂ molecules
48 suppress the pz rotation in both LS and HS frameworks. As a result, the
49 rotational entropy difference between the HS and the LS frameworks is negligibly
50
51
52
53
54
55
56
57
58
59
60
61
62
63
64
65

1
2
3
4
5
6
7
8
9 small in the CS₂ clathrate. This leads to Eq. 8.

$$\Delta S_{\text{guest-free}} - \Delta S_{\text{CS}_2 \text{ clathrate}} \approx \Delta S_{\text{rot}}. \quad (8)$$

10
11
12
13
14
15 Note that spin (or orbital) entropy terms of the guest-free PCP and the CS₂
16
17 clathrate are cancelled out in the left-hand side of Eq. 8. This is because the
18
19 vdW interaction between CS₂ and the PCP framework little influences the spin
20
21 and the orbital degeneracies of each state. From Eqs. 1, 7, and 8, the $T_{1/2}$ shift
22
23 is derived as

$$\Delta T_{1/2} \equiv T_{1/2}^{\text{CS}_2 \text{ clathrate}} - T_{1/2}^{\text{guest-free}} \approx \frac{\Delta H_{\text{guest-free}} \Delta S_{\text{rot}}}{\Delta S_{\text{guest-free}} (\Delta S_{\text{guest-free}} - \Delta S_{\text{rot}})}. \quad (9)$$

24
25
26 A previous experiment reported $\Delta H_{\text{guest-free}} = 6.05 \text{ kcal mol}^{-1}$ and $\Delta S_{\text{guest-free}}$
27
28 $= 20.3 \text{ cal mol}^{-1} \text{ K}^{-1}$ for single crystal $\{\text{Fe}^{\text{II}}(\text{pz})[\text{Pt}^{\text{II}}(\text{CN})_4]\}$ [3]. Thus, the
29
30 $T_{1/2}$ shift was calculated to be 29.7 K with Eq. 9. This large shift agrees
31
32 well with the experimental results that the $T_{1/2}$ of the CS₂ clathrate ($T_{1/2} >$
33
34 330 K) is significantly higher than that of the guest-free PCP ($T_{1/2}^{\downarrow} = 285 \text{ K}$
35
36 and $T_{1/2}^{\uparrow} = 309 \text{ K}$) [4]. This agreement shows that the loss of ΔS_{rot} from
37
38 $\Delta S_{\text{guest-free}}$ caused by the CS₂ binding with pz ligands is crucial for the CS₂-
39
40 induced HS→LS transition. Although the experiment of the HS→LS transition
41
42 by the CS₂ adsorption was carried out with powder PCP [2, 4], the discussion
43
44 of $T_{1/2}$ is little different between powder and single crystal PCP (see supporting
45
46 content on page 6).

47
48
49
50
51
52 The $T_{1/2}$ shift by guest adsorption is explained in a more general way (Figure
53
54 6). In the guest-free PCP (Figure 6a), the LS state is the ground state at low
55
56 temperature. As temperature increases, the increase in $T\Delta S^{\text{HS-LS}}$ term stabi-

1
2
3
4
5
6
7
8
9 lizes the HS state because ΔS^{HS-LS} is positive. Hence, the LS→HS transition
10 occurs at the $T_{1/2}$. When bulky molecules or many molecules are adsorbed, the
11 HS state becomes the ground state even at low temperature because the HS
12 state provides large pores to decrease the steric repulsion between bulky guests
13 and the PCP framework. Hence, ΔH^{HS-LS} becomes negative. This means that
14 the ΔG^{HS-LS} line is shifted to negative even at low temperatures (Figure 6b).
15 In CS₂ clathrate, ΔS^{HS-LS} becomes smaller than the guest-free PCP, which
16 decreases the slope of the ΔG^{HS-LS} line. Thus, the $T_{1/2}$ value shifts to higher
17 temperature than in the guest-free PCP (Figure 6c).
18
19
20
21
22
23
24
25
26
27
28
29

30 *3.4. Origin of the potential energy barriers of pyrazine rotation*

31

32 As discussed in Sec. 3.1, the potential energy of pz rotation becomes maxi-
33 mum when the pz ligand is parallel to the Fe – NC bonds (Figures 3a and S2).
34 The rotation of pz ligands around the Fe – Fe axes can induce changes in the
35 steric repulsion between the pz ligand and CN⁻ anions and the π -back donation
36 between Fe d_π , namely d_{yz} and d_{zx} , and pz π^* orbitals (Figure S5); remember
37 that the π -back donation is weaker in the HS state than in the LS one because
38 only one d_π orbital is doubly occupied in the HS state (Figure S6). These would
39 be the origin of rotational energy barriers in the LS and the HS states. In the
40 pz and the NH₃ models (Figures 2c and 2d), the PECs of the LS state show
41 almost the same barriers (Figures 3b) of 3.2 kcal mol⁻¹. If the energy barrier
42 arose from the back-donation, the barrier should disappear in the NH₃ model,
43 because the back-donation in the NH₃ model occurs at the same extent even
44
45
46
47
48
49
50
51
52
53
54
55
56
57
58
59
60
61
62
63
64
65

1
2
3
4
5
6
7
8
9 when the pz ligand rotates (Figure S5a). Remember that two d_π (d_{yz} and d_{zx})
10 orbitals are degenerate in the $\text{Fe}(\text{NH}_3)(\text{NC})_4$ moiety but not in the $\text{Fe}(\text{pz})(\text{NC})_4$
11 moiety (Figure S5). Also similar energy barrier ($2.8 \text{ kcal mol}^{-1}$) was calculated
12 in a model including a Zn(II) cation instead of the Fe(II) cation. In this Zn
13 model, the back-donation is not formed at all between Zn(II) and the pz ligand.
14
15 These results indicate that the back-donation is not responsible for the barrier.
16
17
18
19
20

21 The steric repulsion between the pz ligand and the Fe – NC bonds is larger
22 at $\theta = \pi/4$ rad than at $\theta = 0$ rad. The difference in the steric repulsion be-
23 tween $\theta = 0$ and $\pi/4$ rad is larger in the LS framework than in the HS one
24 because the Fe – pz distance is shorter in the LS framework than in the HS
25 one [3, 4]. Hence, the barrier is higher in the LS framework than in the HS
26 one (Figures 3a and S2). From these results, it is concluded that the steric
27 repulsion is the origin of the rotation barrier. We wish to mention here that
28 the multi-reference wave function presents better computational results because
29 of complicated electronic structure of the Fe(II) moiety but the present results
30 by the DFT(B3LYP) method are sufficient to provide semi-quantitative under-
31 standing at least (see supporting content on pages 9-10).
32
33
34
35
36
37
38
39
40
41
42
43
44
45
46

47 **4. Conclusions**

48
49
50 We investigated the mechanism of the CS_2 -induced HS→LS transition of
51 $\{\text{Fe}^{\text{II}}(\text{pz})[\text{Pt}^{\text{II}}(\text{CN})_4]\}$, considering hindered rotational entropy of the pz lig-
52 ands. In the guest-free PCP, pz ligands rotate much easier in the HS framework
53 than in the LS one because the steric repulsion in the HS framework is weaker
54
55
56
57
58

1
2
3
4
5
6
7
8
9 than in the LS one. Thus, the entropy difference (ΔS_{rot}) between the HS and
10 the LS states is positive. In CS₂ clathrate, however, CS₂ molecules are strongly
11 adsorbed between pz ligands to suppress the pz rotation and to decrease ΔS_{rot} .
12 We evaluated the ΔS_{rot} value and estimated how much $T_{1/2}$ shifts through
13 the CS₂ adsorption. The results indicate that the decrease in ΔS_{rot} induces
14 the HS→LS transition. All computational results and discussion are consistent
15 with the experimental ones. This is the first clear understanding of the $T_{1/2}$
16 shift based on the entropy difference between the HS and the LS states.
17
18
19
20
21
22
23
24
25
26
27

28 Acknowledgements

29
30
31 This work was financially supported by the Ministry of Education, Culture,
32 Sports, Science and Technology through Grants-in-Aid for Specially Promoted
33 Research (No. 22000009), Scientific Research (No. 23245014), and JSPS Fel-
34 lows (No. 208230). Some of the electronic structure calculations were performed
35 with Altix4700 and PRIMEQUEST workstations of the Institute for Molecular
36 Science (Okazaki, Japan).
37
38
39
40
41
42
43
44
45

46 References

- 47
48
49 [1] V. Niel, J.M. Martinez-Agudo, M.C. Muñoz, A.B. Gaspar, J.A. Real, Inorg.
50 Chem. 40 (2001) 3838.
51
52
53
54 [2] S. Bonhommeau, G. Molnár, A. Galet, A. Zwick, J.-A. Real, J.J. McGarvey,
55 A. Bousseksou, Angew. Chem. Int. Ed. 44 (2005) 4069.
56
57
58

1
2
3
4
5
6
7
8
9
10
11
12
13
14
15
16
17
18
19
20
21
22
23
24
25
26
27
28
29
30
31
32
33
34
35
36
37
38
39
40
41
42
43
44
45
46
47
48
49
50
51
52
53
54
55
56
57
58
59
60
61
62
63
64
65

[3] S. Cobo, D. Ostrovskii, S. Bonhommeau, L. Vendier, G. Molnár, L. Salmon, K. Tanaka, A. Bousseksou, *J. Am. Chem. Soc.* 130 (2008) 9019.

[4] M. Ohba, K. Yoneda, G. Agustí, M.C. Muñoz, A.B. Gaspar, J.A. Real, M. Yamasaki, H. Ando, Y. Nakao, S. Sakaki, S. Kitagawa, *Angew. Chem. Int. Ed.* 48 (2009) 4767.

[5] C.P. Slichter, H.G. Drickamer, *J. Chem. Phys.* 56 (1972) 2142.

[6] P. Gütllich, H. Köppen, R. Link, H.G. Steinhäuser, *J. Chem. Phys.* 70 (1979) 3977.

[7] A.D. Becke, *J. Chem. Phys.* 98 (1993) 5648.

[8] C. Lee, W. Yang, R.G. Parr, *Phys. Rev. B: Condens. Matter* 37 (1988) 785.

[9] B. Miehlich, A. Savin, H. Stoll, H. Preuss, *Chem. Phys. Lett.* 157 (1989) 200.

[10] M. Dolg, U. Wedig, H. Stoll, H. Preuss, *J. Chem. Phys.* 86 (1987) 866.

[11] T.H. Dunning, Jr., *J. Chem. Phys.* 90 (1989) 1007.

[12] R.A. Kendall, T.H. Dunning, Jr., R.J. Harrison, *J. Chem. Phys.* 96 (1992) 6796.

[13] G.G. Balint-Kurti, C.L. Ward, C.C. Marston, *Comput. Phys. Commun.* 67 (1991) 285.

[14] S.F. Boys, F. Bernardi, *Mol. Phys.* 19 (1970) 553.

- 1
2
3
4
5
6
7
8
9 [15] M. Reiher, *Inorg. Chem.* 41 (2002) 6928.
10
11 [16] H. Paulsen, L. Duellund, A. Zimmermann, F. Averseng, M. Gerdan, H.
12 Winkler, H. Toftlund, A.X. Trautwein, *Monatsh. Chem.* 134 (2003) 295.
13
14
15
16 [17] H. Paulsen, J.A. Wolny, A.X. Trautwein, *Monatsh. Chem.* 136 (2005) 1107.
17
18
19 [18] P. Gütlich, H.A. Goodwin, *Top. Curr. Chem.* 233 (2004) 1.
20
21
22
23
24
25
26
27
28
29
30
31
32
33
34
35
36
37
38
39
40
41
42
43
44
45
46
47
48
49
50
51
52
53
54
55
56
57
58
59
60
61
62
63
64
65

1
2
3
4
5
6
7
8
9
10
11
12
13
14
15
16
17
18
19
20
21
22
23
24
25
26
27
28
29
30
31
32
33
34
35
36
37
38
39
40
41
42
43
44
45
46
47
48
49
50
51
52
53
54
55
56
57
58
59
60
61
62
63
64
65

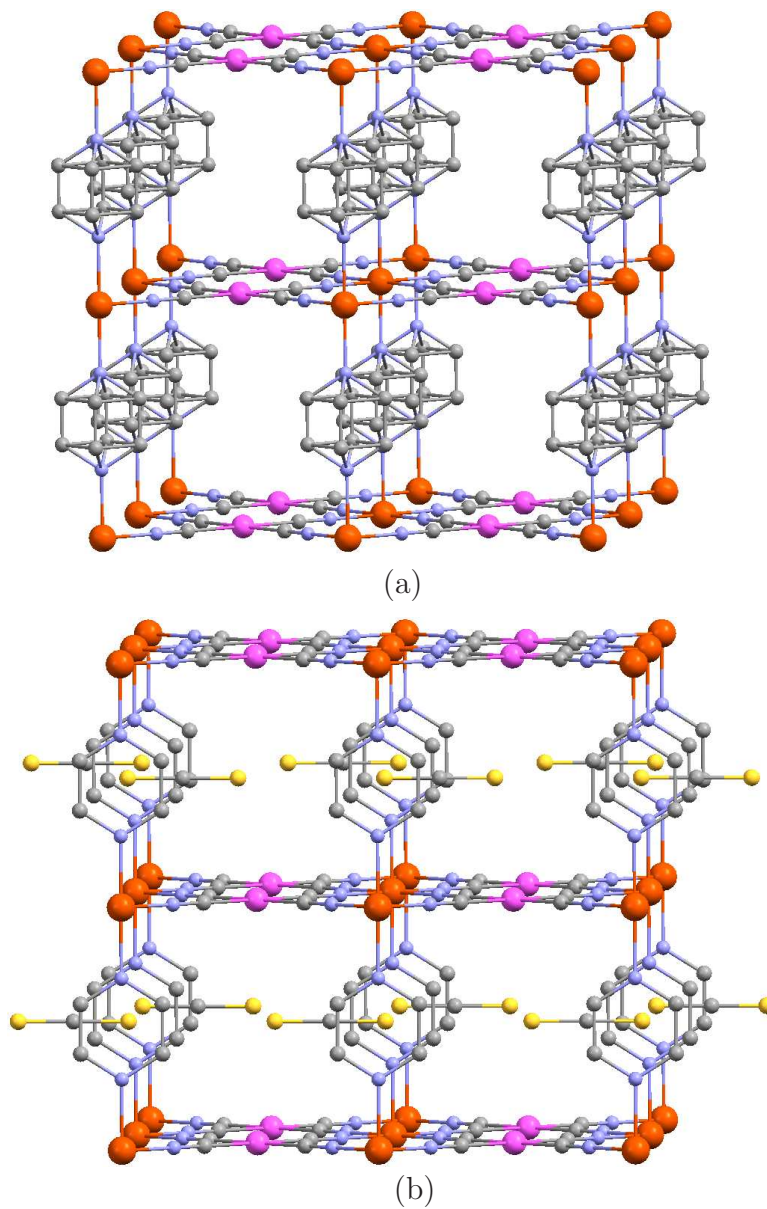


Figure 1: Crystal structures of (a) guest-free framework of $\{\text{Fe}^{\text{II}}(\text{pz})[\text{Pt}^{\text{II}}(\text{CN})_4]\}$ and (b) CS_2 clathrate obtained with the X-ray diffraction measurement [4]. Fe (orange), Pt (pink), N (purple), C (gray), and S (yellow).

1
2
3
4
5
6
7
8
9
10
11
12
13
14
15
16
17
18
19
20
21
22
23
24
25
26
27
28
29
30
31
32
33
34
35
36
37
38
39
40
41
42
43
44
45
46
47
48
49
50
51
52
53
54
55
56
57
58
59
60
61
62
63
64
65

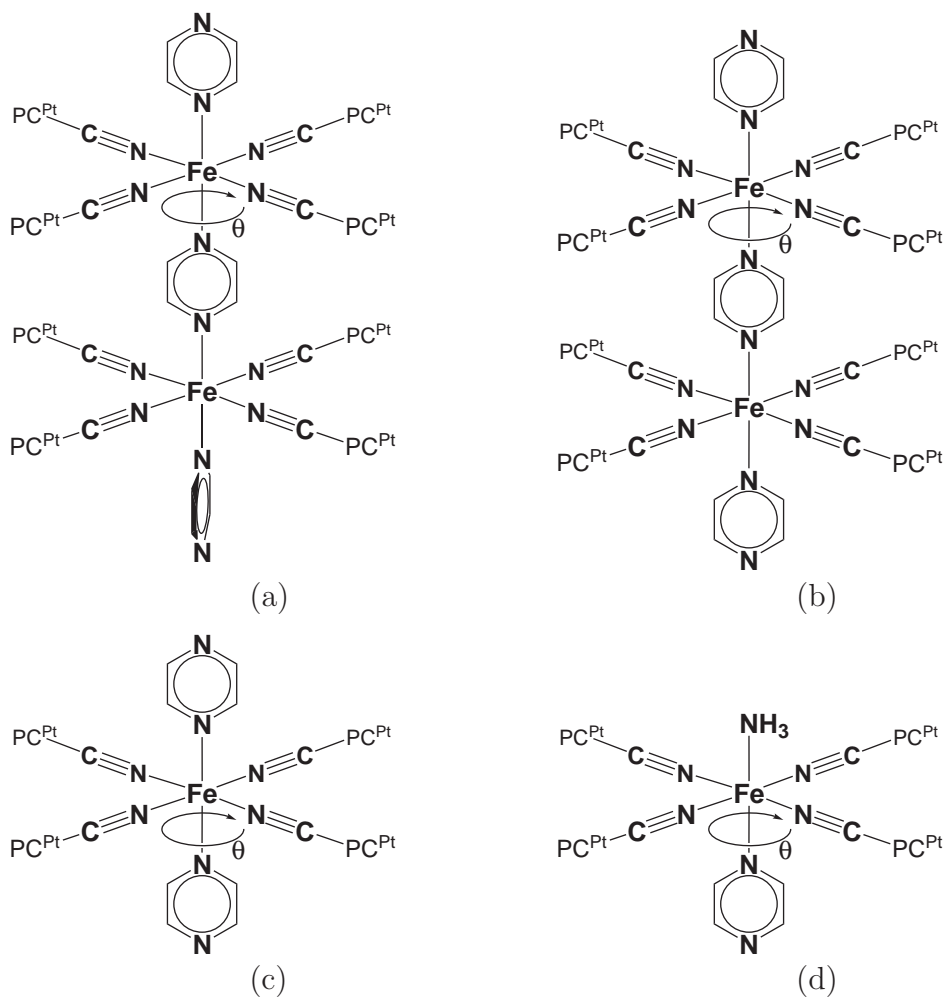
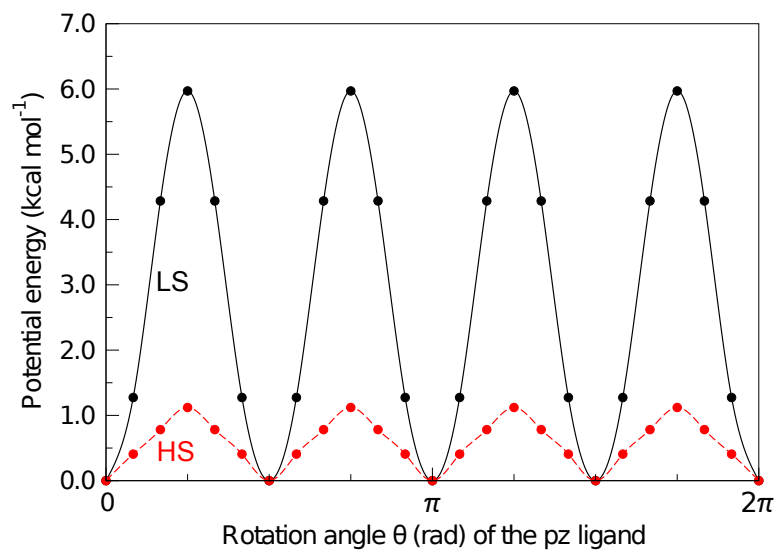
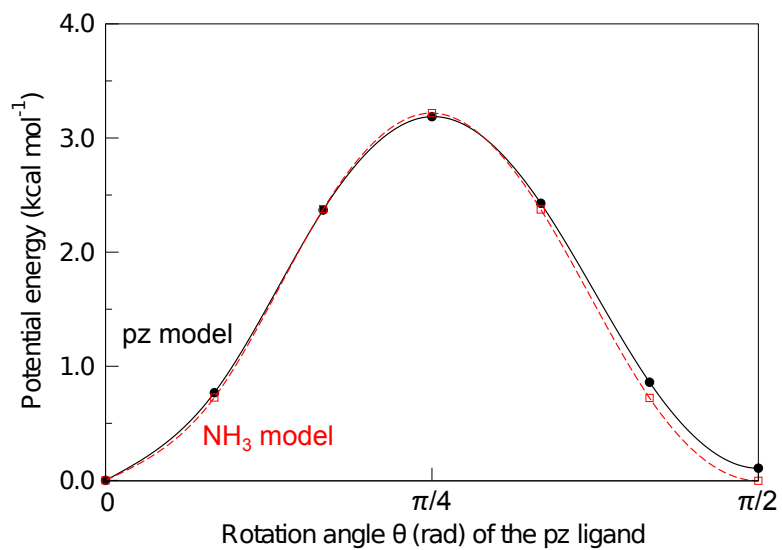


Figure 2: Local structure models employed to investigate the potential energy curves of p_z hindered rotation: (a) vertical model, (b) parallel model, (c) p_z model, and (d) NH₃ model. Point charges (PC^{Pt}) of +0.5 e are placed to mimic the Pt centers.



(a)



(b)

Figure 3: Potential energy curves of pz hindered rotation: (a) vertical model and (b) pz model vs. NH₃ model in the LS state. In all models, the energy at $\theta = 0$ rad is set to be zero.

1
2
3
4
5
6
7
8
9
10
11
12
13
14
15
16
17
18
19
20
21
22
23
24
25
26
27
28
29
30
31
32
33
34
35
36
37
38
39
40
41
42
43
44
45
46
47
48
49
50
51
52
53
54
55
56
57
58
59
60
61
62
63
64
65

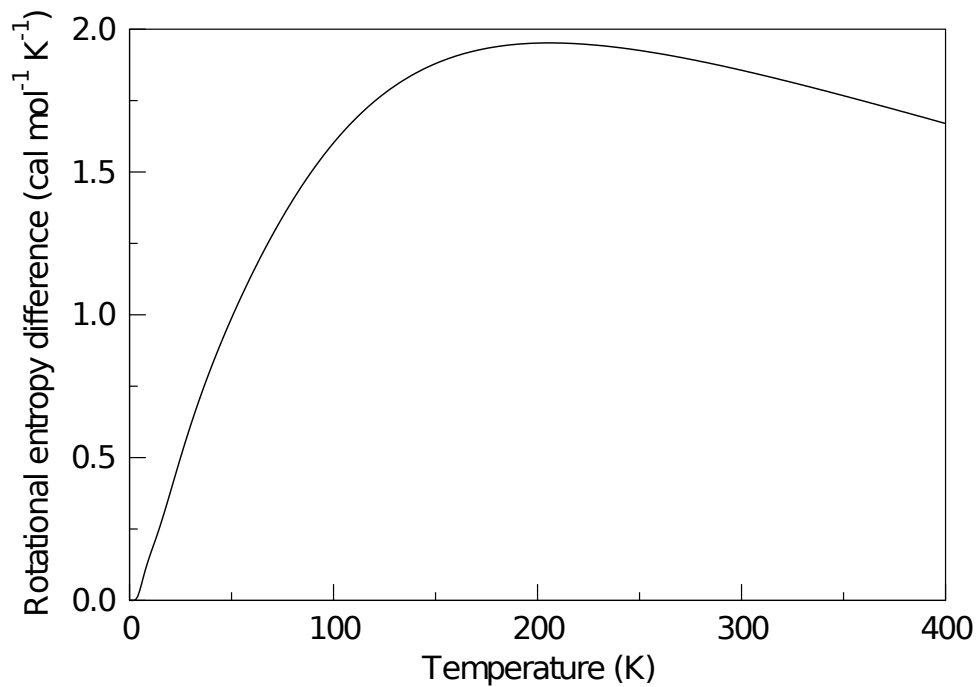
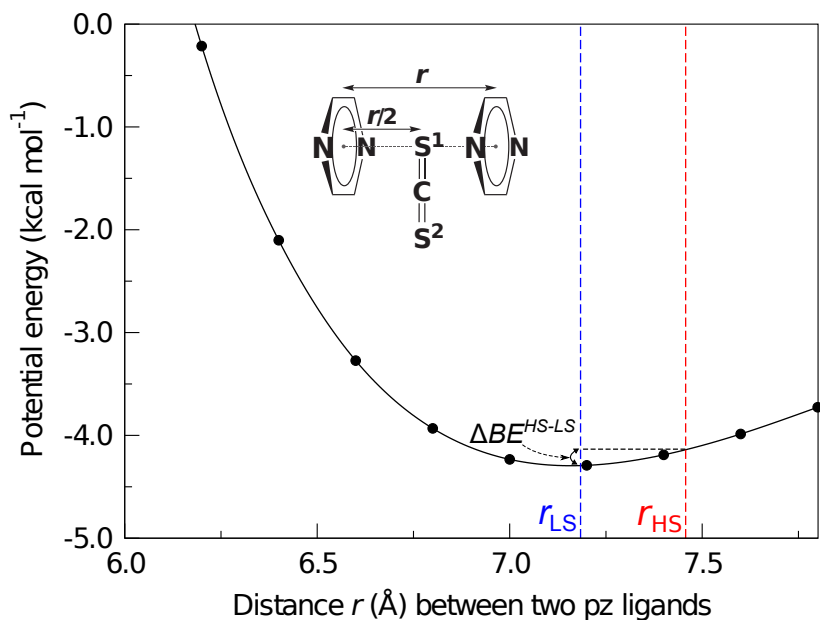
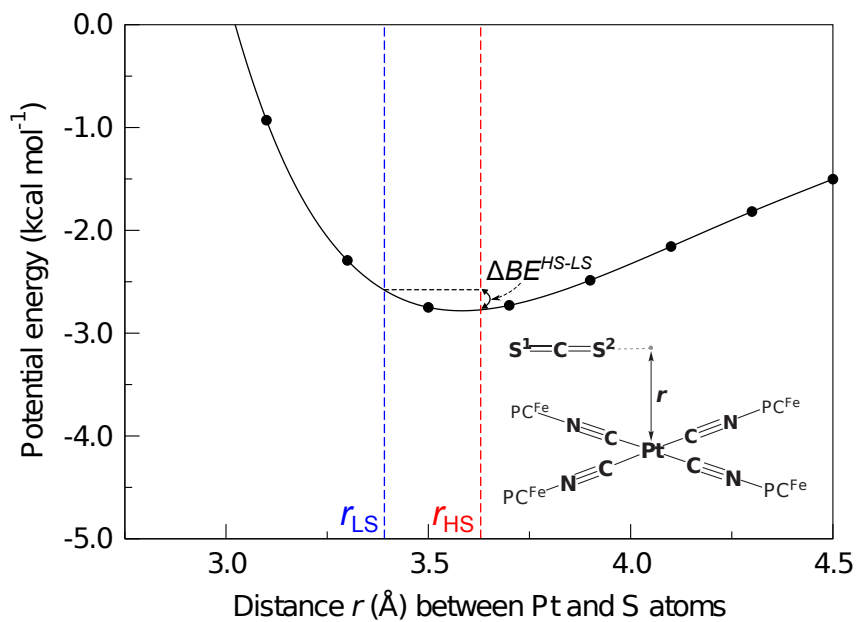


Figure 4: Difference (ΔS_{rot}) between hindered rotational entropy of pz ligands in the HS framework and that in the LS framework. The vertical model (Figure 2a) is employed because the PECs of the vertical model are similar to those of the parallel one.



(a)



(b)

Figure 5: Potential energy curves for the interaction of CS_2 at (a) site A and (b) site B. The binding energies at site B discussed in the text are estimated to be double the value in Figure 5b because CS_2 interacts with two Pt atoms at site B (see Figure 1b). The r_{LS} and r_{HS} values represent the corresponding distances in the experimental LS and HS frameworks, respectively. Point charges (PC^{Fe}) of $+0.5 e$ are placed to mimic the Fe centers.

1
2
3
4
5
6
7
8
9
10
11
12
13
14
15
16
17
18
19
20
21
22
23
24
25
26
27
28
29
30
31
32
33
34
35
36
37
38
39
40
41
42
43
44
45
46
47
48
49
50
51
52
53
54
55
56
57
58
59
60
61
62
63
64
65

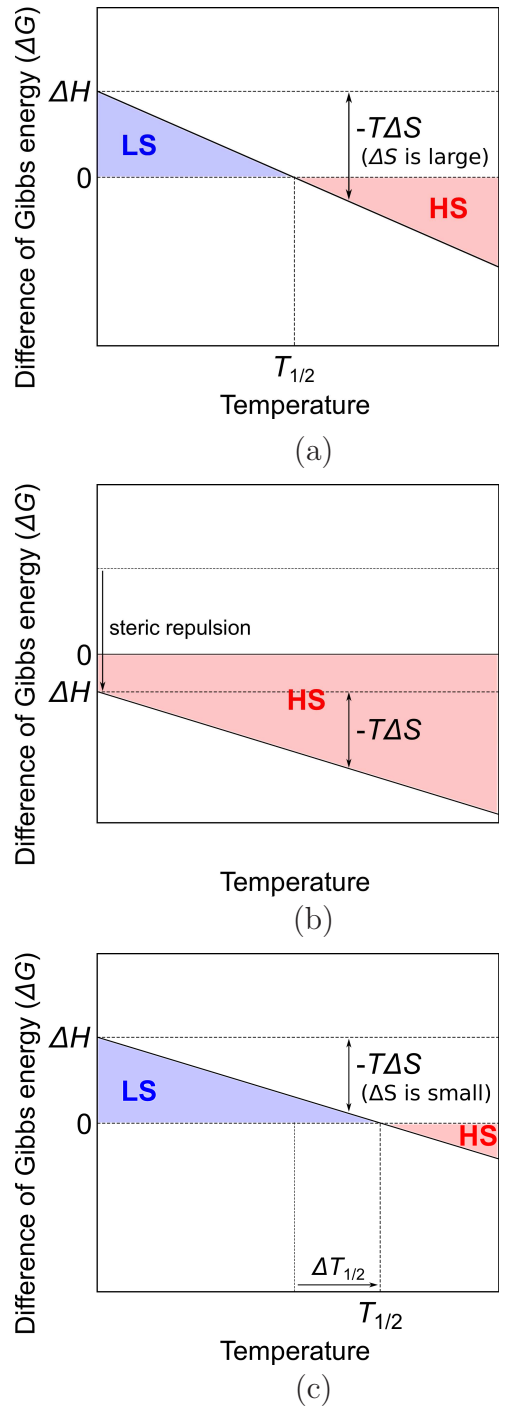


Figure 6: Schematic interpretation of the change in spin transition temperature ($T_{1/2}$): (a) guest-free or small molecule clathrate, (b) large or many-adsorbed molecule clathrate, and (c) CS_2 clathrate. The difference of Gibbs energy is defined as follows: $\Delta G^{HS-Ls} \equiv \Delta H^{HS-Ls} - T\Delta S^{HS-Ls}$.

Supplementary Content for
“Theoretical Study on High-Spin to Low-Spin
Transition of {Fe(pyrazine)[Pt(CN)₄]}: Guest-Induced
Entropy Decrease”

Hideo Ando^a, Yoshihide Nakao^a, Hirofumi Sato^a, Masaaki Ohba^b, Susumu
Kitagawa^c, Shigeyoshi Sakaki^{d,*}

^a*Department of Molecular Engineering, Graduate School of Engineering, Kyoto University,
Nishikyo-ku, Kyoto 615-8510, Japan*

^b*Department of Chemistry, Graduate School of Sciences, Kyushu University, Hakozaki
Higashi-ku, Fukuoka 812-8581, Japan*

^c*Department of Synthetic Chemistry and Biological Chemistry, Graduate School of
Engineering, Kyoto University, Nishikyo-ku, Kyoto 615-8510, Japan*

^d*Fukui Institute for Fundamental Chemistry, Kyoto University, Takano-Nishihiraki-cho,
Sakyo-ku, Kyoto 606-8103, Japan*



*Corresponding author. Tel: +81 75 7117907. Fax: +81 75 7114757.

Email addresses: hideo@tich14.mbox.media.kyoto-u.ac.jp (Hideo Ando),
nakao.yoshihide.5a@kyoto-u.ac.jp (Yoshihide Nakao), hirofumi@moleng.kyoto-u.ac.jp
(Hirofumi Sato), ohba@chem.kyushu-univ.jp (Masaaki Ohba),
kitagawa@icems.kyoto-u.ac.jp (Susumu Kitagawa),
sakaki@qmst.mbox.media.kyoto-u.ac.jp (Shigeyoshi Sakaki)

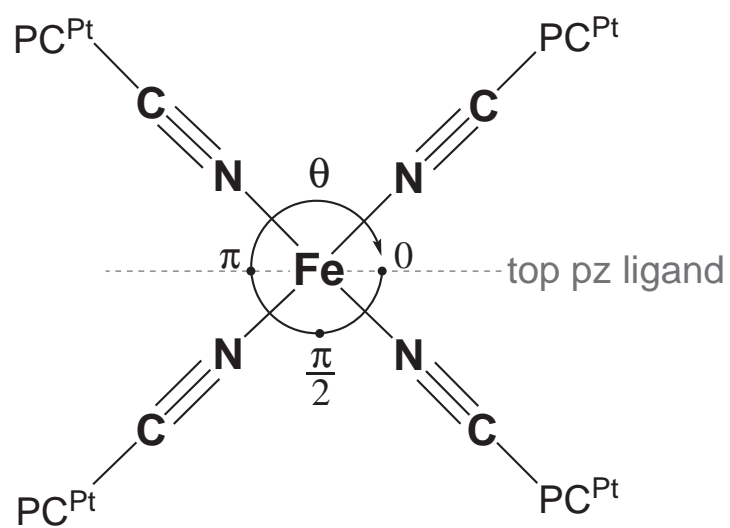


Figure S 1: Definition of the rotation angle θ (top view) of middle pz ligand in the local structure models employed (Figure 2). Point charges (PC^{Pt}) of $+0.5 \epsilon$ are placed to mimic the Pt centers.

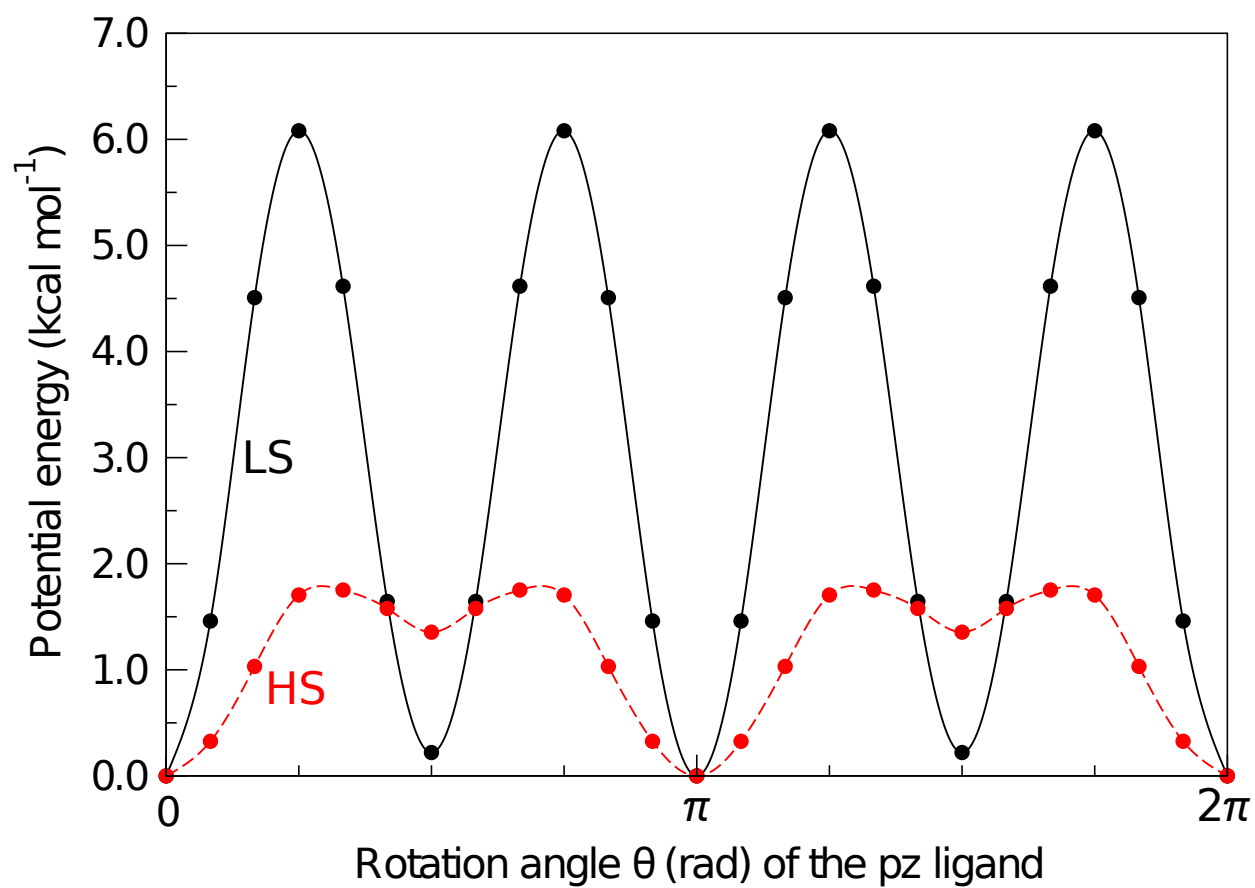


Figure S 2: Potential energy curves of pz hindered rotation in the parallel model (Figure 2b). The energy at $\theta = 0$ rad is set to be zero.

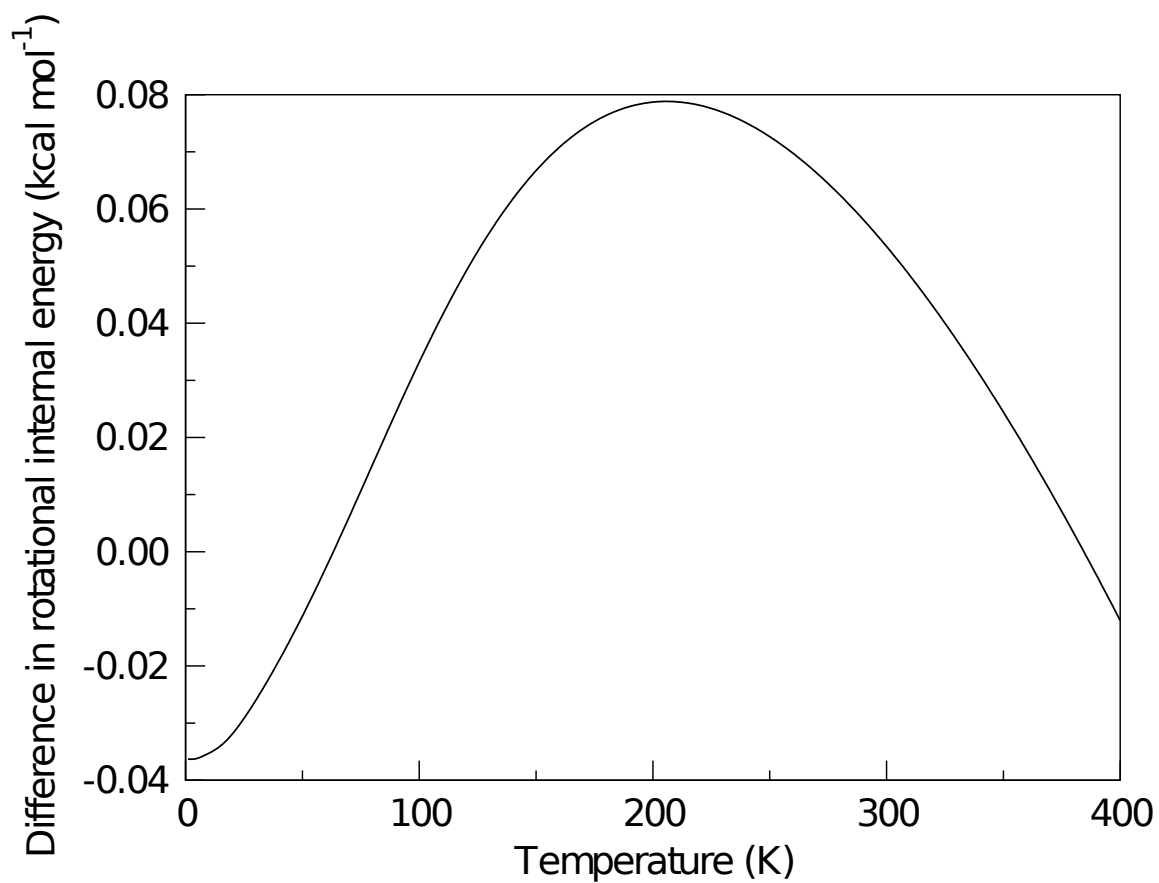


Figure S 3: Difference (ΔU_{rot}) between rotational internal energy of pz ligands in the HS framework and that in the LS framework. The vertical model (Figure 2a) is employed because the PECs of the vertical model are similar to those of the parallel one.

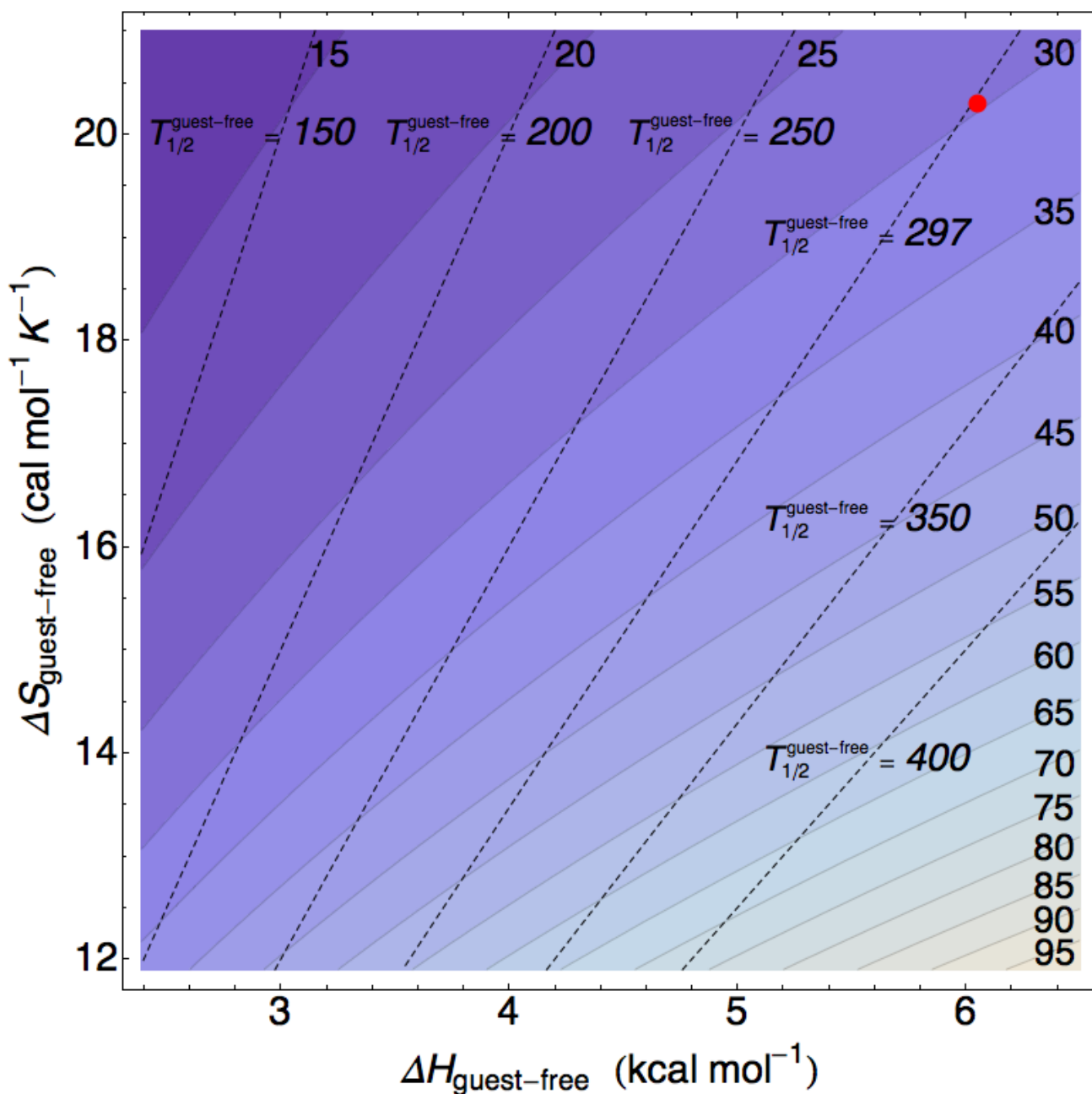


Figure S 4: Contour plot of the CS_2 -induced $T_{1/2}$ shift in kelvin (K). Dashed lines with italic numbers ($T_{1/2}^{\text{guest-free}}$) represent guest-free PCPs whose spin transition temperature is equal to $T_{1/2}^{\text{guest-free}}$ K. For example, single crystal $\{\text{Fe}^{\text{II}}(\text{pz})[\text{Pt}^{\text{II}}(\text{CN})_4]\}$ is represented by the red dot near the dashed line with 297, which indicates that the $T_{1/2}$ shift is 29.7 K. The plot area covers typical values of ΔH ($2.39 - 4.78 \text{ kcal mol}^{-1}$) and ΔS ($11.9 - 19.1 \text{ cal mol}^{-1} \text{K}^{-1}$) in spin-crossover compounds [19].

Estimation of CS₂-Induced $T_{1/2}$ Shift in Powder of $\{\text{Fe}^{\text{II}}(\text{pz})[\text{Pt}^{\text{II}}(\text{CN})_4]\}$

Although $\Delta H_{\text{guest-free}}$ and $\Delta S_{\text{guest-free}}$ in powder PCP [2, 4] are not exactly the same as those in single crystal PCP [3], the difference is not essential to the arguments in Sec. 3.3. The experimental $\Delta H_{\text{guest-free}}$ and $\Delta S_{\text{guest-free}}$ values are not reported in the powder PCP [4]. However, the $T_{1/2}$ shift can be discussed from a contour plot of the $T_{1/2}$ shift (Figure S4), which was obtained with Eq. 9. The plot area covers typical ΔH and ΔS values in spin-crossover compounds [19]. The red dot in Figure S4 corresponds to the values of the single crystal PCP [3]. Guest-free PCPs with a certain transition temperature, $T_{1/2}^{\text{guest-free}}$, corresponds to the dashed line (Figure S4). The powder PCP has a transition temperature of *ca.* 297 K ($= (T_{1/2}^{\downarrow} + T_{1/2}^{\uparrow})/2$) in the absence of CS₂. From the dashed line with 297 K in the plot area (Figure S4), it is clear that the powder PCP also exhibits the $T_{1/2}$ shift from *ca.* 28 K to *ca.* 54 K through CS₂ adsorption. In general, when guest adsorption decreases $\Delta S_{\text{guest-free}}$, guest-free PCPs which have higher $T_{1/2}^{\text{guest-free}}$ exhibit larger $T_{1/2}$ shift.

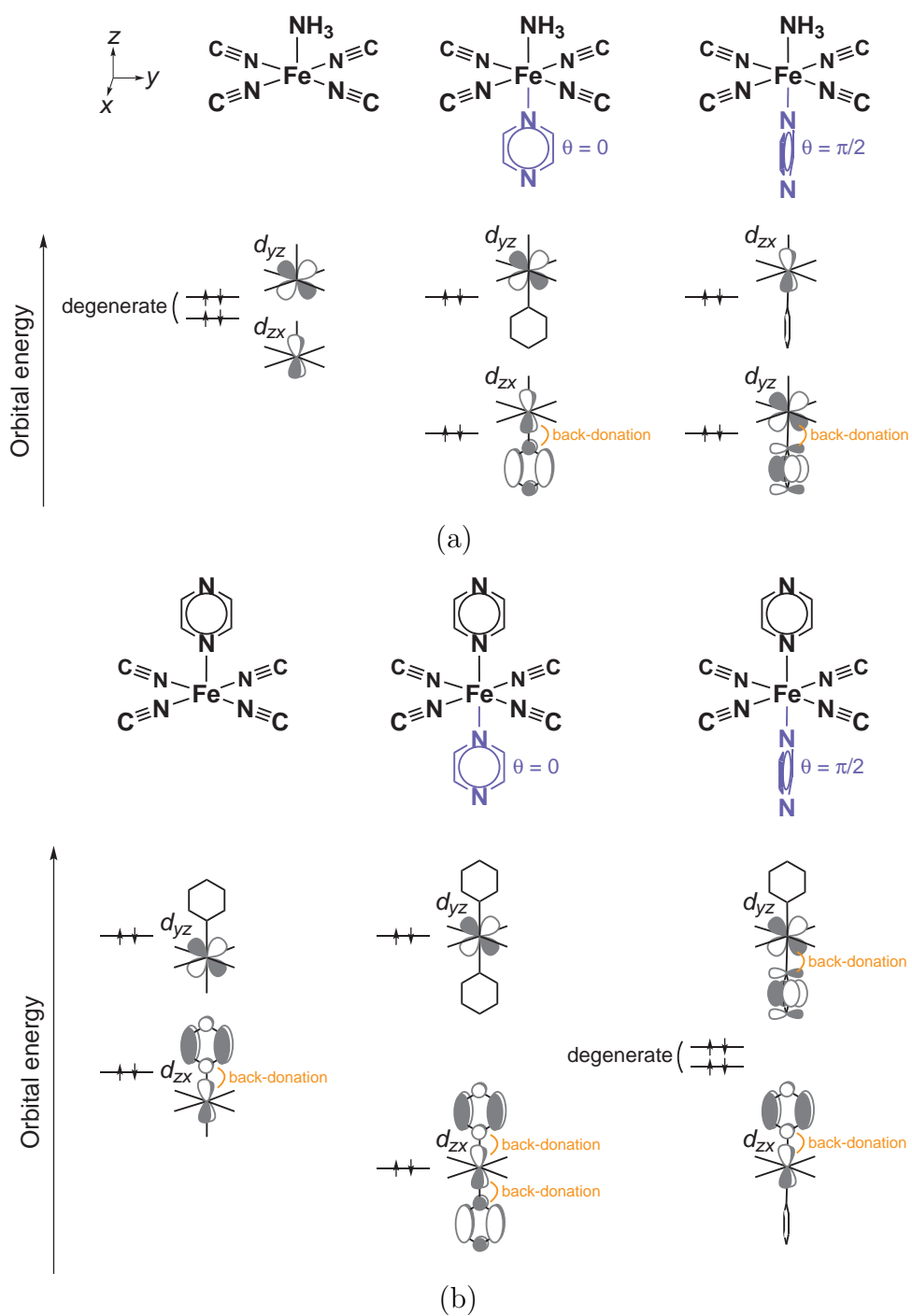


Figure S 5: Schematic orbital energy splitting due to π -back donation between Fe d_π (d_{yz} and d_{zx}) and $p_z \pi^*$ orbitals: (a) NH₃ model and (b) pz model. Because the two d_π orbitals are degenerate in the Fe(NH₃)(NC)₄ moiety, back-donation in the NH₃ model occurs at the same extent even when the p_z ligand rotates. 7

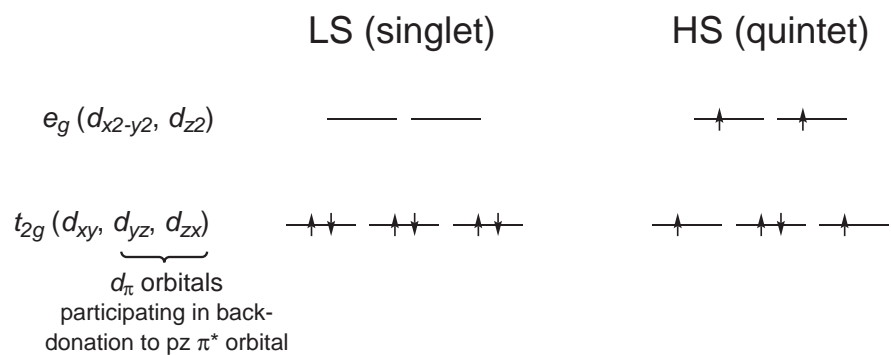


Figure S 6: Schematic electron configurations of the LS and the HS state. In the HS state calculated with the DFT(B3LYP) method, the d_{xy} orbital is singly occupied.

Validity of the Use of the DFT Method To Investigate Potential Energy Curves of the Pyrazine Rotation

Weak points of the DFT(B3LYP) method such as lack of non-dynamical correlation and vdW interactions may influence the computational results of PECs of the pz rotation. We examined how much these weak points influence our results and discussion.

In the LS state, there is no low-lying excited state; in fact, we did not find instability in the wave function of the LS state, suggesting that single-reference method can be used here. In the HS state, there are several near-degenerate states, indicating that we had better to use multi-reference method. However, we employed the DFT(B3LYP) method because multi-reference *ab initio* calculation could not be carried out due to high computational cost. The use of single-reference method is not unreasonable, as follows: We focus here on the PECs of the pz rotation. It is likely that the PECs along the Fe–Fe and the Fe–pz distances are considerably influenced by the use of multi-reference method, but the PECs for the pz rotation are not influenced very much by the use of multi-reference method because the origin of its energy barrier is steric repulsion with the CN[−] ligands, as discussed in Sec. 3.4.

To ascertain our discussion above, we employed another local structure model (Fe-absent model), which is similar to the pz model (Figure 2c) but does not include the Fe atom. In this Fe-absent model, non-dynamical correlation does not exist. The barrier height of the Fe-absent model obtained by the DFT(B3LYP) method is 2.8 kcal/mol for the LS geometry and 0.5 kcal/mol

for the HS geometry. These barrier heights agree with those of the pz model including the Fe atom; 3.2 kcal/mol for the LS state and 0.9 kcal/mol for the HS state. This good agreement indicates that the barrier mainly arises from steric repulsion with the CN^- ligands. It is likely that the use of single-reference method is acceptable for investigation of the pz rotation.

There remains another problem: The DFT(B3LYP) method does not always present correct steric repulsion because it fails to evaluate the vdW interaction. We evaluated here the barrier heights with the MP4 method in the Fe-absent model. The calculated barrier heights are close to those obtained with the the DFT(B3LYP) method; 3.2 kcal/mol for the LS geometry and 0.6 kcal/mol for the HS one.

All these results indicate that the DFT(B3LYP)-calculated PECs are useful to present semi-quantitative discussion, at least.